1990-08-15

Environmental effects on acoustic measures of global ocean warming

Semtner, A.J. Jr.; Chervin, R.M.

Journal Name: Journal of Geophysical Research; (USA); Journal Volume: 95:C8
http://hdl.handle.net/10945/61044

JOURNAL OF GEOPHYSICAL RESEARCH, VOL. 95, NO. C8, PAGES 12,973–12,982, AUGUST 15, 1990

Environmental Effects on Acoustic Measures of Global Ocean Warming

ALBERT J. SEMTNER, JR.

Naval Postgraduate School, Monterey, California

ROBERT M. CHERVIN

National Center for Atmospheric Research, Boulder, Colorado

Munk and Forbes (1989) have proposed an acoustic technique for measuring the ocean warming caused by the buildup of greenhouse gases in the atmosphere. Travel time from a source in the South Indian Ocean will be monitored at receivers as far away as the North Atlantic and North Pacific. However, there are natural perturbations of acoustic travel time over long distances as a result of oceanic mesoscale eddies, seasonal fluctuations, and interannual variability. Results from a global eddy-resolving ocean model are used here to assess the importance of two of these noise factors. Neither mesoscale nor seasonal effects are found to be large enough to obscure the anticipated signal of global change in the ocean. Analyses of the modeled temperature trends and variability along three selected paths give insights into where mesoscale and seasonal variability affect the acoustics.

1. INTRODUCTION

The Earth's climate is now widely thought to be undergoing global change as a result of release into the atmosphere of "greenhouse gases" such as carbon dioxide and chlorofluorocarbons. Many uncertainties exist as to (1) the overall magnitude of the response to a prescribed input, (2) the rate at which the response will occur, and (3) the geographic distribution of the response. These in turn are strongly related to poorly understood oceanic processes which govern (1) the uptake of carbon dioxide and other gases by the ocean, (2) the sequestering of excess heat absorbed from the atmosphere in the deep ocean, and (3) the modification of surface temperature as a result of complex changes in ocean heat transport and mixing. Narrowing the level of uncertainty in each of the areas will require extensive modeling of global ocean processes in order to predict global climate change.

Of equal importance to the problem of predicting climate change is the problem of monitoring climate change. By monitoring climate change, we will not only have a better idea of what is happening but also be able to "validate" models for global change and increase our confidence in their predictions. However, attempts to measure climate change on land and at the sea surface encounter their own uncertainties which relate to instrument errors, changes in instrumentation, inadequate sampling, and geophysical "noise" in the climate system. It becomes highly desirable to have a monitoring technique which avoids these pitfalls as much as possible.

An innovative technique for monitoring ocean warming at middepths, which appears to bypass many of the aforementioned problems, has been proposed by *Munk and Forbes* [1989] (hereinafter referred to as MF). Low-frequency sound pulses of moderate intensity can be detected across vast ocean distances. The travel times of these pulses can be measured with great accuracy, and they constitute "proxy" records of average ocean temperature along the paths. It thus becomes possible in principle to measure both the sequestering of heat in the ocean and, if sufficient transmitters and receivers are involved, the spatial distribution of the temperature changes. However, it is important to assess the extent to which geophysical noise may complicate the problem. In the case of sound in the ocean, geophysical noise can originate in internal waves, mesoscale eddies, seasonal fluctuations, and multiyear variations. As was discussed by MF, this noise can affect both the path by which sound travels between two specified points and the speed at which it travels.

The present study has been undertaken to evaluate the levels of geophysical noise that arise in the ocean as a result of mesoscale and seasonal variability. (No treatment of path changes and long-term fluctuations is undertaken at this time.) The approach uses an existing eddy-resolving numerical model of the global ocean [*Semtner and Chervin*, 1988] (hereinafter referred to as SC). That model has been integrated for many years both with annual mean surface forcing and with monthly varying forcing. The output from the model constitutes a "proxy" data set for actual ocean conditions, and the method of MF can be tested using the model output along selected paths.

Section 2 of this note describes the SC global ocean model and its simulated variability. Three paths specified by MF for analysis of mesoscale and seasonal noise are exhibited. Section 3 describes the results of the analysis, and section 4 has conclusions and suggestions for further work.

2. THE GLOBAL DATA SET

The SC ocean model was constructed in order to make possible realistic simulations of global ocean circulation and climate using the best available supercomputers. The physical and numerical features of the model are on a par with the best models that have been formulated over two decades at the NOAA Geophysical Fluid Dynamics Laboratory in Princeton, New Jersey, while the computational features are significantly enhanced. Some important scientific and computational considerations in the developmental effort are described by *Semtner and Chervin* [1990]. A design phase of

Paper number 90JC00642.
0148-0227/90/90JC-00642$05.00

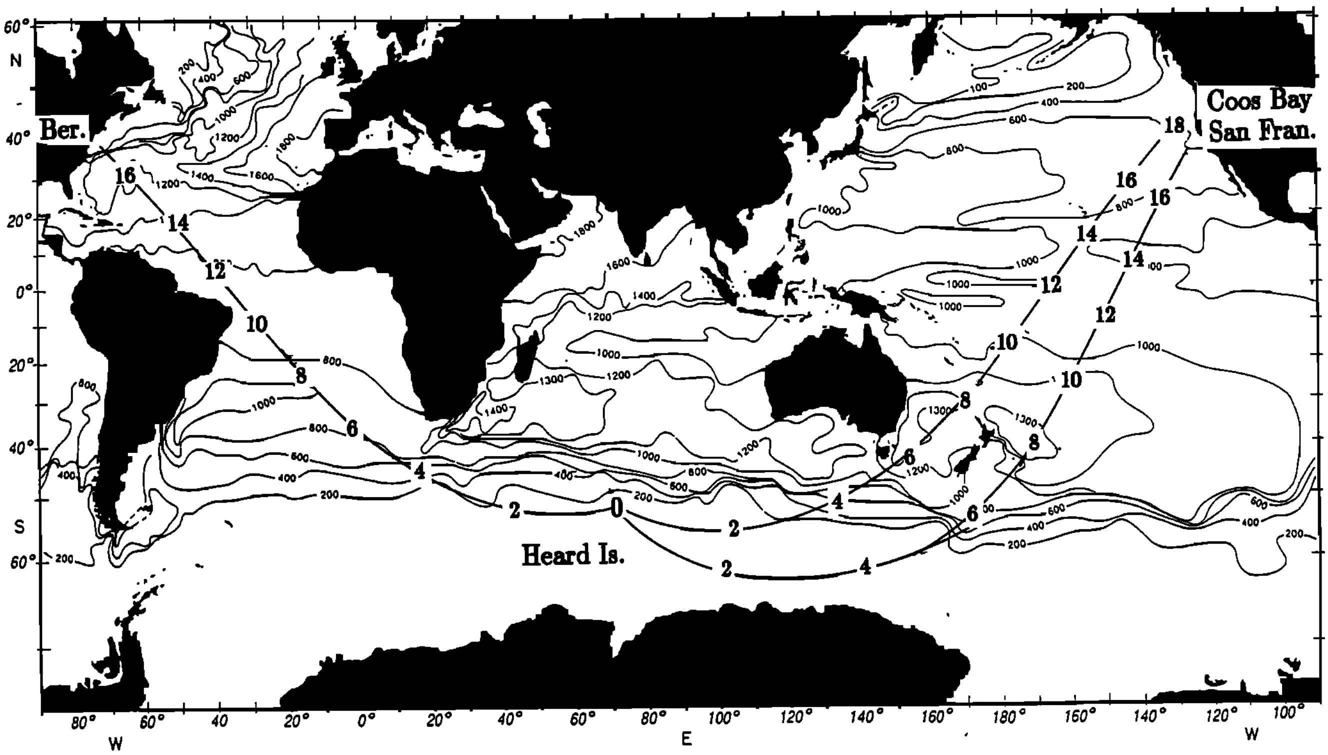

Fig. 1. The acoustic paths from Heard Island in the South Indian Ocean to Bermuda, Coos Bay, and San Francisco. Detailed prescriptions of these paths were provided for the present study by W. H. Munk and A. M. G. Forbes (personal communication, 1989). Distance markers are shown every 2000 km. The paths are superimposed on *Munk and Forbes'* [1989] figure of the depth of the sound channel in meters.

model optimization for supercomputers having many processors was followed by a construction phase for global modeling. In the latter phase, coastlines, bottom topography, gridded temperature and salinity data of *Levitus* [1982], and wind stress from *Hellerman and Rosenstein* [1983] were prepared for straightforward use in the model with any chosen horizontal grid spacings and vertical grid structure.

A Cray X-MP/48 was available to the authors in 1987 at the National Center for Atmospheric Research (NCAR). On this machine, grid spacings of 0.5° in the horizontal and 20 levels in the vertical were computationally feasible while allowing entry into the regime of resolved eddies. A logical first calculation was done to spin up the general circulation of the model to a quasi-steady, annual mean state. Eddies were temporarily suppressed by the use of Laplacian friction in order to allow an accelerated method of time stepping. The deep ocean was weakly constrained to the observed temperature and salinity structure, but the thermocline was free to come into equilibrium with the surface forcing (as in the study of *Sarmiento and Bryan* [1982]). Following this 18-year spin-up, continuing integrations with resolved eddies were carried out, first with annual mean forcing and then with monthly forcing, for a total simulated time of 30 years. This follow-on 12-year integration used biharmonic mixing and standard time stepping. Model output was archived every 3 simulated days during years 20–30 for subsequent analysis. It is this model output that fortuitously provides the only existing "proxy data" for evaluating the mesoscale and seasonal levels of environmental noise on a global basis.

To indicate briefly the nature of the model results, Plate 1 shows 2.5-year standard deviations of temperature at the depths of 160, 310, and 610 m. (Plate 1 can be found in the separate color section in this issue.) These are for the period of constant annual mean forcing and show only the intrinsic mesoscale variability in the model. Many instabilities that are evident here are also found in the observed variability from Seasat measurements of surface height, as reported by *Cheney et al.* [1983]. Some of the instability regions are examined by SC. The strongly unstable currents of both the model and the real ocean include the Gulf Stream, the Kuroshio/Oyashio, the East Australia Current, the Brazil/Falkland (Malvinas) Confluence, the Agulhas Current, and the Antarctic Circumpolar Current. The model and Seasat results have comparable regions of variability in certain tropical areas, such as in the North Equatorial Current and Countercurrent of the Pacific and in the North Brazil Current.

The mesoscale-only variability at the depths 160, 310, and 610 m has typical magnitudes of 1.0°, 0.5°, and 0.2°C in strong current areas. Since equivalent maps of observed variability without seasonal effects do not exist, it is hard to judge how realistic these levels are. We suspect they are

Fig. 2. (Opposite) Simulated (left) travel times and (right) path-averaged temperatures from Heard Island to (top) Coos Bay, (middle) San Francisco, and (bottom) Bermuda. Ten years of model output at 3-day intervals were available as an extension to the 20-year integration of *Semtner and Chervin* [1988]. The first 2.5 years were with annual mean forcing, and the remaining 7.5 years were with monthly mean forcing. In the latter case, each integral year marker represents July 1. Light curves show times and temperatures every 3 days, while the heavy curves show the results of making 360-day running averages. Boldface numerals give rms differences between the curves.

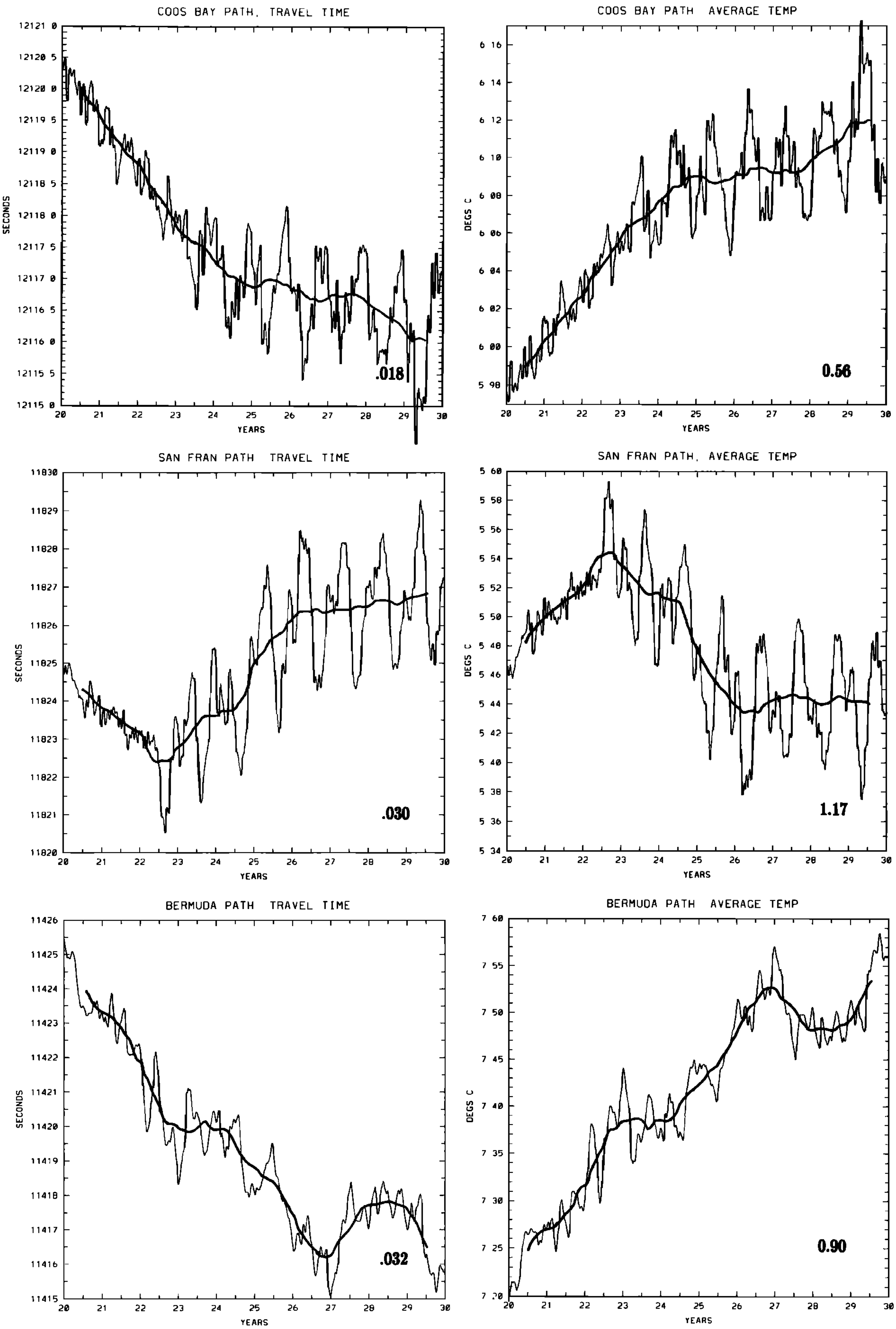
COOS BAY PATH, TRAVEL TIME
SECONDS
YEARS
.018
COOS BAY PATH AVERAGE TEMP
DEGS C
YEARS
0.56
SAN FRAN PATH TRAVEL TIME
SECONDS
YEARS
.030
SAN FRAN PATH, AVERAGE TEMP
DEGS C
YEARS
1.17
BERMUDA PATH TRAVEL TIME
SECONDS
YEARS
.032
BERMUDA PATH AVERAGE TEMP
DEGS C
YEARS
0.90

within a factor of 2, and we expect higher-resolution model studies to give more accurate estimates in the future.

As shown in the polar projection of Plate 2, the Antarctic Circumpolar Current has many elongated zones of variability along its path. (Plate 2 can be found in the separate color section in this issue.) These coincide roughly with topographic features such as mid-ocean ridges and rises and more isolated barriers such as the Macquarie Rise, the Campbell Plateau, the Kerguelen Islands, and the Scotia Ridge. The Agulhas and Brazil/Falkland Current areas are also very active. In general, variability in stream function matches that in each of the temperature plots, with variability of temperature decreasing with depth.

Many of the unstable currents mentioned can affect the acoustic monitoring plan of MF. Three paths are shown in Figure 1 from Heard Island in the Indian Ocean to key receiving stations which will be located in Bermuda, San Francisco, and Coos Bay during a feasibility experiment in early 1991. These paths pass through many of the instability areas evident in Plates 1 and 2. Nearly half of each path is contained within the south polar projection of Plate 2.

Munk and Forbes (personal communication, 1989) have provided the authors with the coordinates every 500 km for the acoustic ray paths shown in Figure 1. These paths follow the depth of the sound velocity minimum. They are refracted in the horizontal by slight lateral variations of sound speed in the sound channel. The paths are only a few hundred meters deep in the high southern latitudes, but descend to about 1-km depth north of 40°S. By mapping these paths into model coordinates, it is possible to perform the experiment of MF in the global model over a fairly long simulated time period. A 10-year portion of the model integration with resolved eddies, with 2.5 years representing annual mean conditions and 7.5 years representing seasonally varying conditions, has been chosen for examination here. Although no external warming has been prescribed for the model, there are internal trends related to annual mean surface forcing during the early years of the integration that can be treated as the signal on which mesoscale and seasonal noise are superimposed.

3. ACOUSTIC RESULTS

Three brief points about methodology are in order:

1. A sequence of horizontal model indices in the 0.5° grid was computed for each of the three paths, along with the depths and segment lengths within boxes. More than 500 boxes were traversed along each path, providing an average along-track length scale of 32 km. As a test of proper algorithm formulation, the sum of the segment lengths along each path was computed and found to be within 0.5% of that determined by the method of MF.

2. The model vertical structure has 12 grid points in the upper 1335 m of the water column. (All but 1% of the total path length resides in the upper 1400 m.) In computations of along-path temperatures and sound velocities, simple linear interpolation between grid point values in the vertical was performed within each horizontal grid box. This procedure leads to somewhat higher temperatures and sound velocities than would occur with higher-order interpolation but should have little effect on the assessment of trends and variabilities. Secondary corrections to sound velocity which involve the pressure of the elevated sea surface and Doppler shifting by currents are ignored. However, the dependence of sound velocity on salinity is retained.

3. For each 3-day time sample, information about temperature and sound velocity along the three paths was computed and saved for later analysis. The processing of 10 simulated years of model output required one pass through 1220 history tapes, each of which represented 2.33 CPU hours of previous Cray X-MP time for a total of nearly 3000 hours.

Figure 2 shows time series of travel time and average temperature for the three paths. (Note that the vertical scales vary for the three paths.) Light lines show 3-day instantaneous values, and heavy lines represent 360-day running averages. A number of things are evident. First, the travel times and the path-averaged temperatures are inverse images of one another, indicating the dominant influence of temperature on sound speed. Subsequent figures will deal with only one field at a time. For easy conversion back and forth, one can use the rule of thumb that a 1.0°C temperature change is equivalent to a 4.0-m/s sound speed change at the depth of the sound channel. Second, the instantaneous records show a transition at 22.5 years from mesoscale-only fluctuations to those which include seasonal oscillations. (It should be noted that year 22.5 represents January 1 of the applied seasonal forcing.) The seasonal fluctuations for Coos Bay appear to be out of phase with those for San Francisco. A 180-day average of temperature for Coos Bay (not shown) indicates that the seasonal cycle peaks about three fourths of the way through the calendar year, at the end of austral winter. Thus the path to Coos Bay warms during austral winter, whereas the path to San Francisco cools at that time. The differing seasonal behavior along the paths could be checked against field measurements made over several seasons.

Both the mesoscale variability and the seasonal cycles are filtered effectively by a 360-day filter. In addition to low-frequency oscillations of small amplitude, the smoothed time series show continuing warming with the use of a seasonal cycle on the Bermuda and Coos Bay paths but a downturn in temperature on the path to San Francisco. The ranges of smoothed temperatures over 9 years are about 0.1°C for Coos Bay and San Francisco and 0.3°C for Bermuda. The first two trends are comparable to previous coarse-grid model estimates of greenhouse warming which are cited by MF. They are likely to be signs of continuing adjustment of the deep thermocline in the Pacific to imposed surface fluxes of heat and moisture. The larger Bermuda trend is probably an indication of continuing adjustment of the South Atlantic region of the eddy-resolving SC model to a vigorous flow of Agulhas waters around the tip of South Africa. The model trends indicate convergence toward a final equilibrium state, since the time series appear to flatten out near the end of the records. In particular, there do not appear to be pronounced multiyear internal fluctuations in the latter parts of the time series. (Externally forced multiyear oscillations such as El Niño are excluded by the prescription of climatological forcing.)

The 3-day time series show extremes of mesoscale fluctuation around the 360-day running mean of about 0.03 degrees, while seasonal plus mesoscale fluctuations are about 0.07 degrees. The combined fluctuations are least pronounced on the Coos Bay path. The fluctuations are most irregular along the Bermuda path.

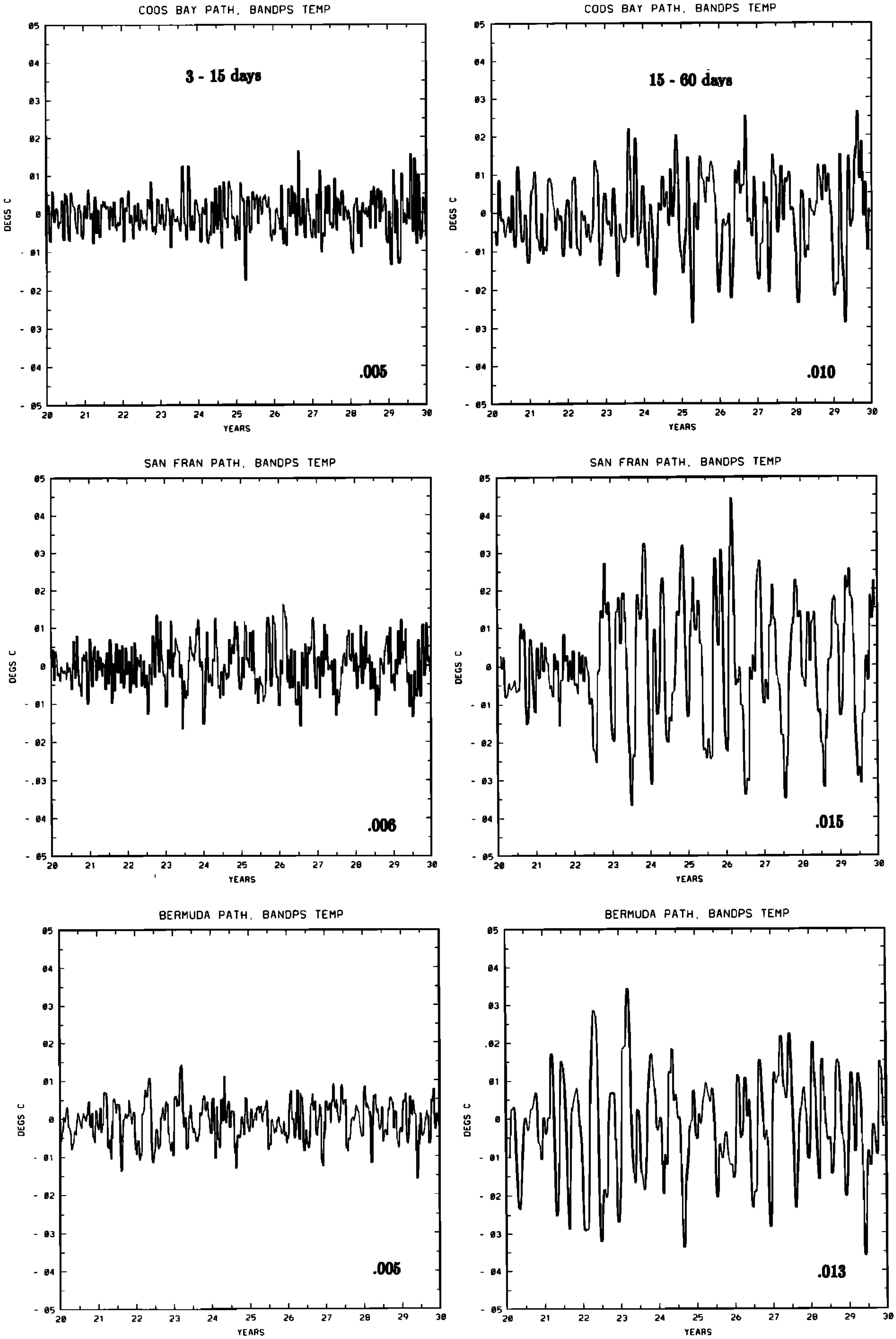

Fig. 3. Decomposition of temperature variability for each path according to increasing time scales of 3–15, 15–60, 60–180, and 180–360 days. The rms norm of each curve is indicated.

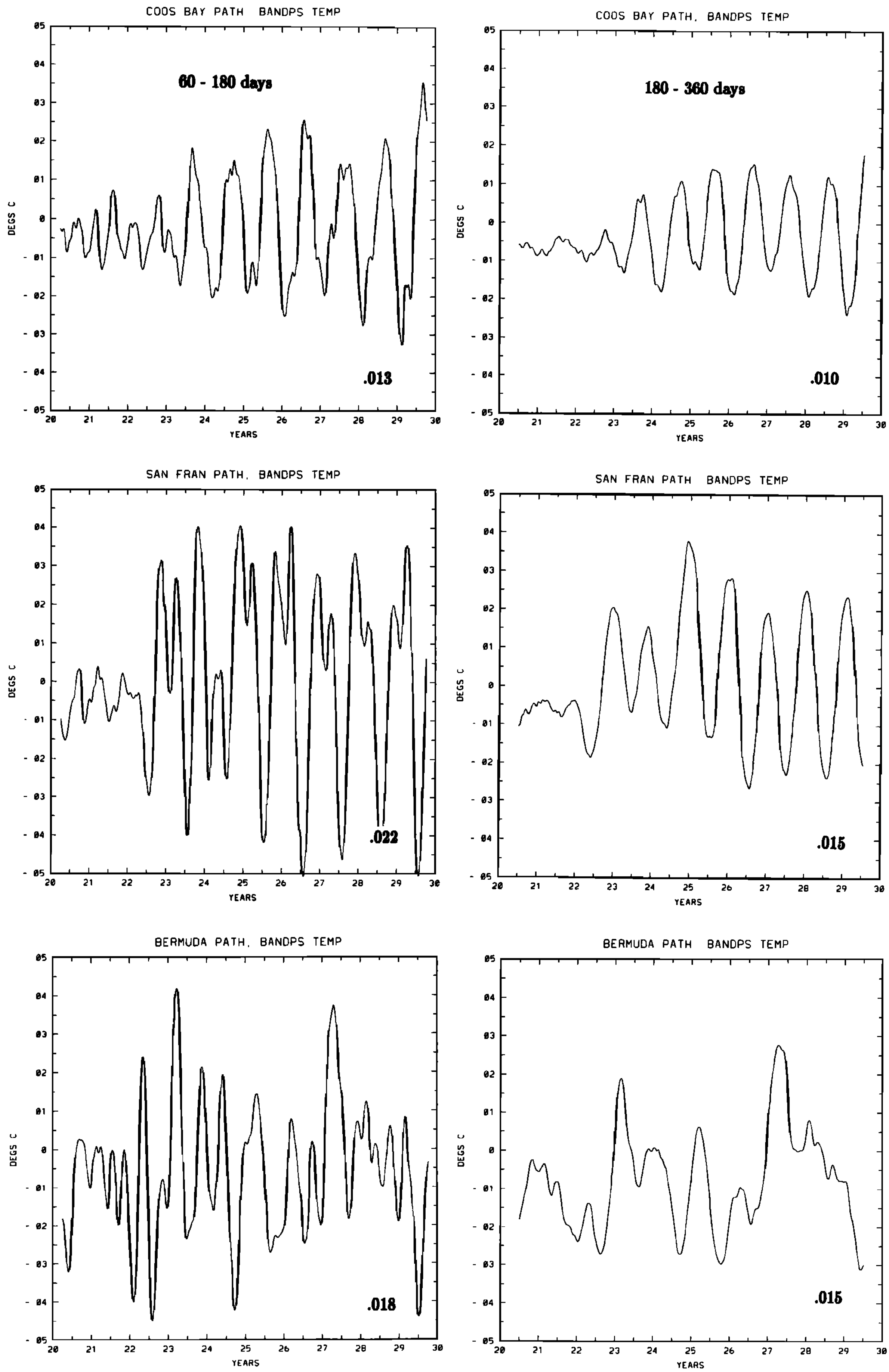

Fig. 3 (continued)

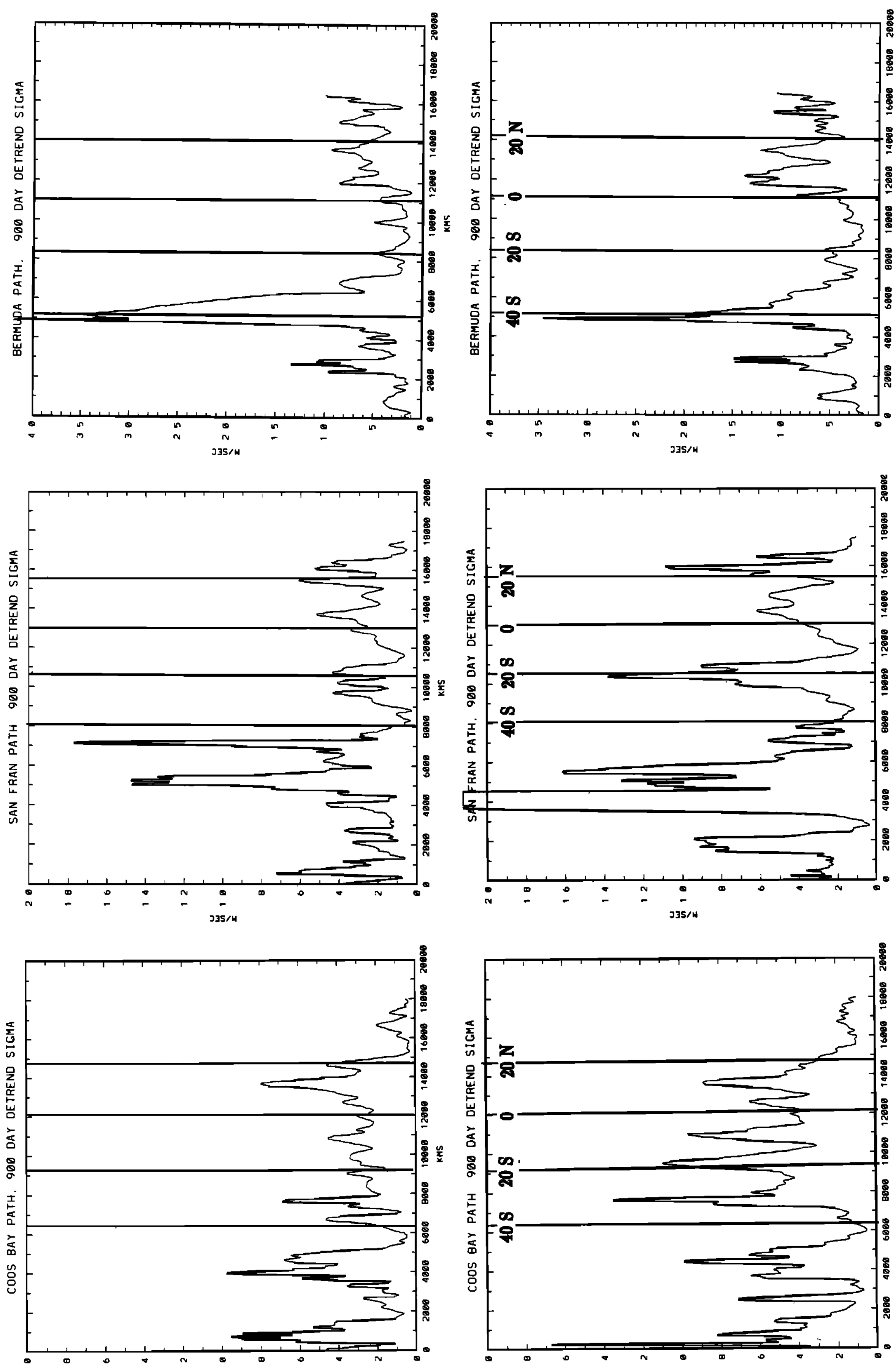

Fig. 4. Along-path standard deviations in sound speed over 2.5-year periods in the (top) annual mean and (bottom) seasonally varying portions of the time series, for (left) Coos Bay, (middle) San Francisco, and (right) Bermuda. Vertical lines indicate latitudes 40°S, 20°S, 0°, and 20°N.

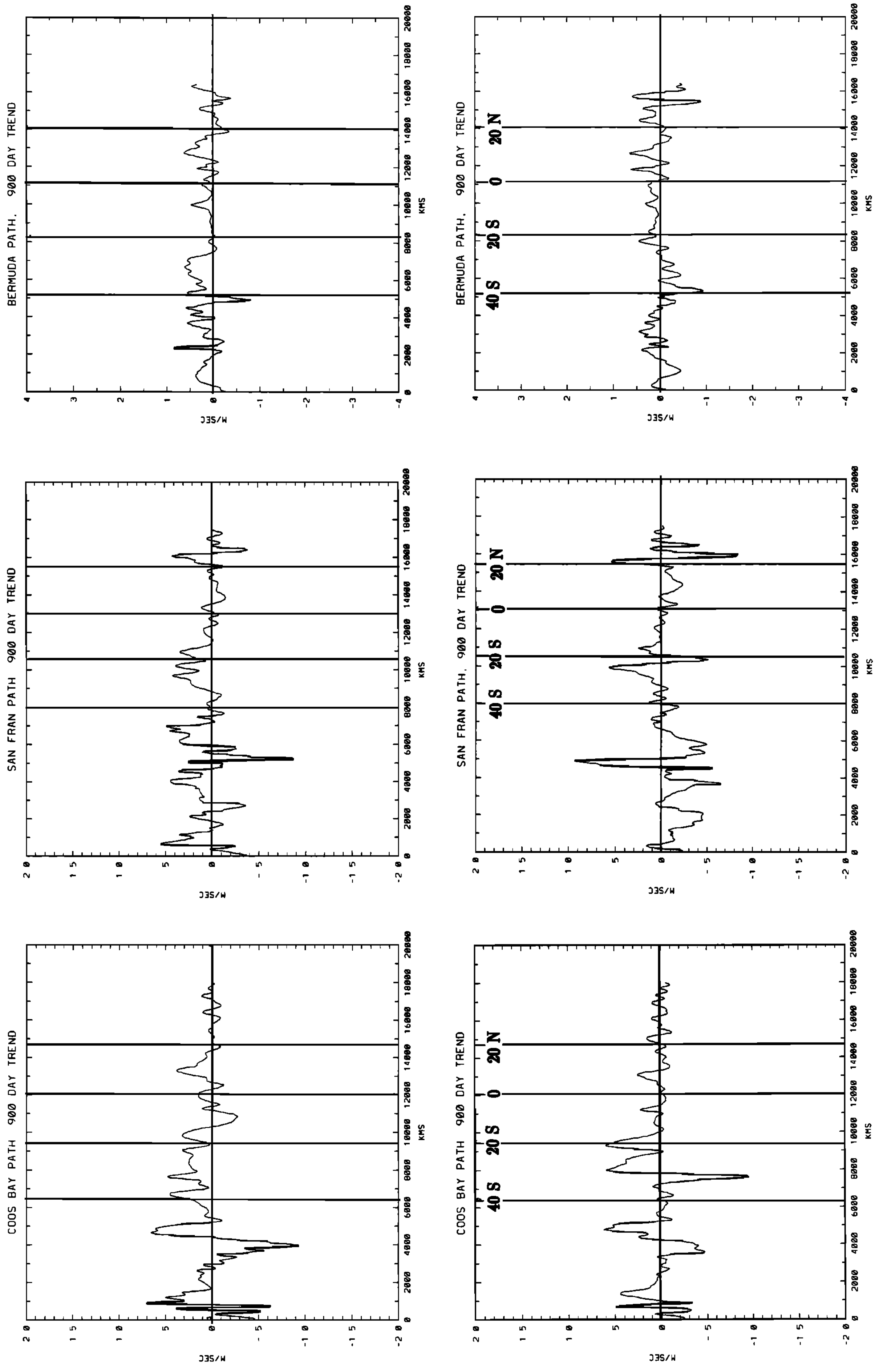

Fig. 5. As in Figure 4, but for the changes of along-path sound speed during the same periods.

Figure 3 gives a breakdown of the temperature variability along the three paths into different frequency ranges. A uniform vertical scale is used. The curves are obtained by subtracting pairs of temperature records that have been averaged over intervals of 3, 15, 60, 180, and 360 days, and they represent roughly the effects of high-frequency, tropical mesoscale, mid-latitude mesoscale, and seasonal fluctuations. The rms norms are shown for each record. The largest fluctations by time scale are in the 60- to 180-day range, and the smallest fluctuations by path are along the Coos Bay route.

Both the Coos Bay and the Bermuda trends in Figure 2 are nearly monotonic after 360-day smoothing. If we take these behaviors to be fortuitous model analogues of greenhouse warming along paths through the Pacific and Atlantic Oceans from the Indian Ocean, the trends would be noticeable over the 10-year record even if greenhouse warming signals were one-half or even one-fourth the magnitude indicated. It thus appears that the technique of MF would be able to detect greenhouse warming.

To give a better understanding of the variability that arises in the time series, Figure 4 shows the standard deviation of sound speed as a function of distance along the three paths. The records have been detrended at each point on the abscissa, and the trends will be examined later. The upper plots are for years 20.0–22.5 of the record with mesoscale eddies, and the lower plots are for years 22.5–25.0 with the added effects of seasonality. The plots have vertical lines indicating the along-track latitudes of 40°S, 20°S, 0°, and 20°N.

The along-track variations in sound speed show a lot of small-scale features, together with ones having intermediate length scales of a few hundred kilometers or broad scales of thousands of kilometers. We do not know how statistically significant the small-scale features are, but their appearance at many of the same locations in both annual mean and seasonal records suggests they represent core regions of meandering currents. A large spike along the Bermuda path is probably indicative of instabilities in the Agulhas region. The intermediate-scale features may be related to wave radiation of energy from some of the unstable currents referred to in section 2, with seasonal enhancements possibly indicating seasonal changes in the strengths of the instabilities. The seasonal enhancements seen between 30°S and 20°N along all three paths may be of this nature. Very broad features of variability which are enhanced by seasonality may be evidence of gyre-scale response to changes in Ekman pumping or suction by surface winds. Finally, some prominent high-latitude zones of seasonal variability along the San Francisco path are probably indicators of convection in the shallow sound channel near Antarctica (see Figure 1).

Figure 5 shows the along-path changes over 2.5 years in sound speed (proportional to temperature) for mesoscale only and for added seasonal conditions. The patterns are complicated and may differ from the large-scale heating patterns such as greenhouse gases would produce, although both represent responses to prescribed forcing. However, there is some basis for agreement in that most panels show minimal effects near the equator and more pronounced effects in the middle and high southern latitudes.

Some adjacent regions of heating and cooling in Figure 5 occur near peaks in the standard deviation curves of Figure 4. These may indicate ongoing redistribution of heat by lateral eddy transports. The average heating in all panels is positive, except for the path to San Francisco when a seasonal cycle exists. In this case, two zones near Antarctica show strong net cooling, presumably as a result of the startup of convection near Antarctica. These regions produce the net cooling along the San Francisco path which was noted in Figure 2.

4. Remarks

The preceding has been a brief examination, using a global eddy resolving model, of the simulated variability in acoustic travel times and average temperatures along three paths. Monitoring of travel time from Heard Island to Bermuda, Coos Bay, and San Francisco has been proposed by *Munk and Forbes* [1989] as a means of measuring global ocean warming. The levels of noise induced by mesoscale ocean eddies and seasonal atmospheric forcing have been found to be sufficiently low that, even without detailed time series analyses, anticipated signals of greenhouse warming should be detectable. Furthermore, a look at the origin of the variability shows the importance of unstable current regions which are found in both the SC model and in satellite observations. Also the importance of low-latitude seasonal changes in the instability properties of strong currents and of high-latitude convection near Antarctica have been suggested. Many of the dynamical phenomena will be further explored by the authors in analyzing the output of the global model in subsequent papers.

A number of additional model studies related to the MF technique are possible. These include determination of possible modifications in the acoustic paths as a result of mesoscale, seasonal, or longer-term thermal fluctuations, experimental design using the model to choose paths with low mesoscale noise, and assessment of how well many stations could diagnose spatial patterns of the heating trends and of the physics of the noise sources. Some of this work is now underway (C.S. Chiu, personal communication, 1990), and three-dimensional ray paths have been computed from the time mean model output and found to follow closely the sound channel trajectories provided by MF. Effects of Doppler shifting by currents are to be examined as well. Application of the MF technique can also be made to subsequent integrations of the global model with interannually varying forcing and with a prescribed buildup of atmospheric fluxes. Finally, further model integrations with increased resolution, both horizontally and vertically, can be carried out for time scales of many decades in order to provide more quantitative representations of both the dynamics and the acoustics. This will be a straightforward task on supercomputers of the 1990s, since the global model has been designed to perform at 10–100 times the speed of a Cray X-MP on such machines.

Acknowledgments. The first author of this paper is supported by grants ATM-8705980 and OCE-8812472 from the National Science Foundation and by contract 079067-A-B1 from Battelle Pacific Northwest Laboratories of the U.S. Department of Energy. The second author is partially supported by a Department of Energy grant from its Carbon Dioxide Research Program to NCAR. Computing resources were provided by the Scientific Computing Division of the National Center for Atmospheric Research. NCAR is sponsored by the National Science Foundation.

REFERENCES

Cheney, R. E., J. G. Marsh, and B. D. Beckley, Global mesoscale variability from Seasat colinear altimeter data, *J. Geophys. Res.*, *88*, 4343–4354, 1983.

Hellerman, S., and M. Rosenstein, Normal monthly wind stress over the world ocean with error estimates, *J. Phys. Oceanogr.*, *13*, 1093–1104, 1983.

Levitus, S., Climatological atlas of the world ocean. *NOAA Prof. Pap. 13*, 173 pp., U.S. Govt. Print. Off., Washington, D.C., 1982.

Munk, W. H., and A. M. G. Forbes, Global ocean warming: An acoustic measure?, *J. Phys. Oceanogr.*, *19*, 1765–1778, 1989.

Sarmiento, J. L., and K. Bryan, An ocean transport model for the North Atlantic, *J. Geophys. Res.*, *87*, 394–408, 1982.

Semtner, A. J., and R. M. Chervin, A simulation of the global ocean circulation with resolved eddies, *J. Geophys. Res.*, *93*, 15,502–15,522, 15,767–15,775, 1988.

Semtner, A. J., and R. M. Chervin, Modeling the ocean with supercomputers—The key to understanding past and future climates, Proceedings of the Global Change Institute on Explaining Records of Past Global Changes, report, edited by J. Eddy, Off. of Interdisciplinary Earth Studies, Univ. Corp. for Atmos. Res., Boulder, Colo., in press, 1990.

R. M. Chervin, National Center for Atmospheric Research, Boulder, CO 80307.

A. J. Semtner, Jr., Department of Oceanography, Naval Postgraduate School, Monterey, CA 93943.

(Received January 26, 1990;
revised February 28, 1990;
accepted March 9, 1990.)

A

B

C

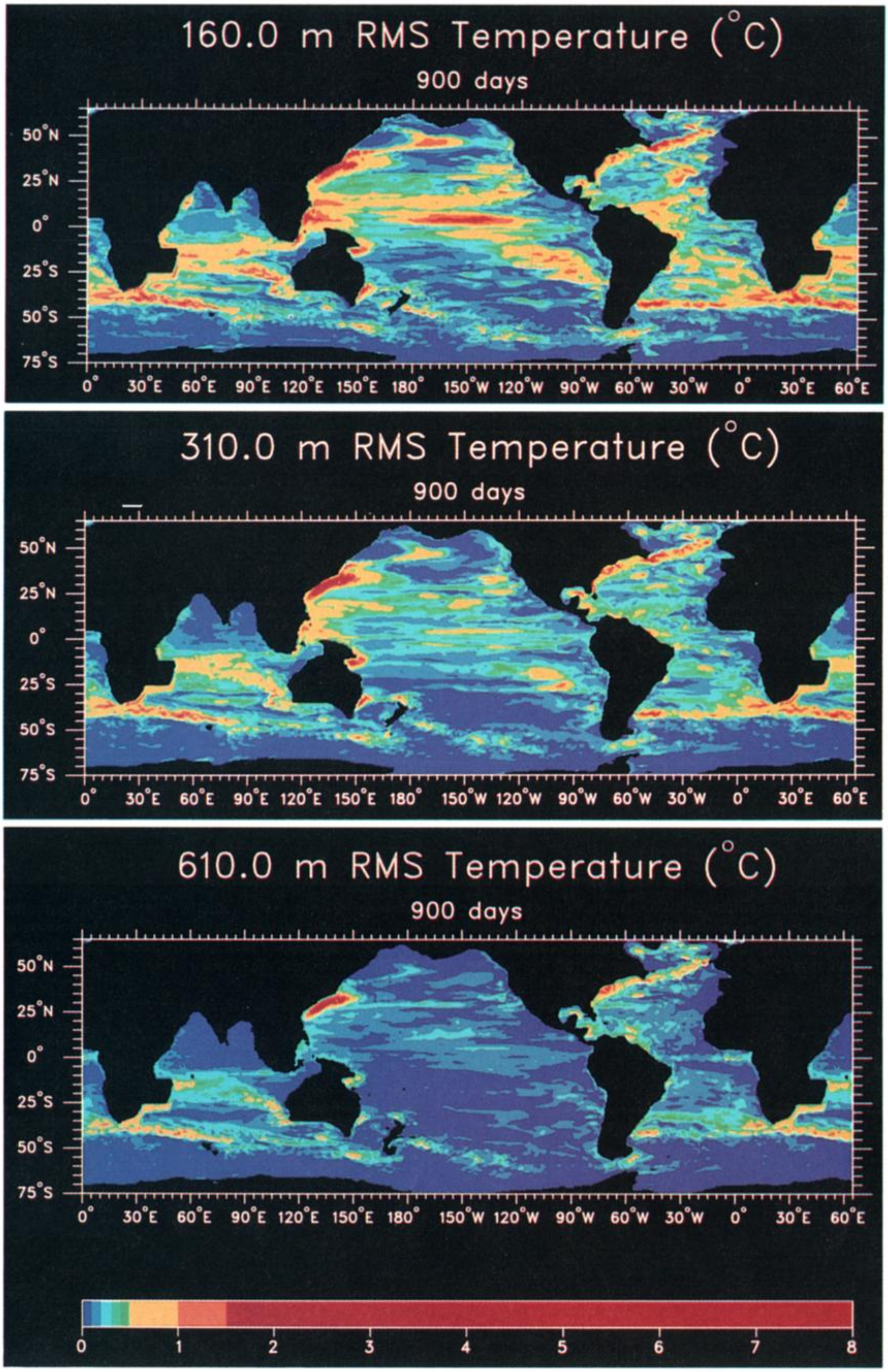

Plate 1 [*Semtner and Chervin*]. Standard deviations of modeled temperature over years 20.0–22.5 of annual mean forcing at depths of (*a*) 160 m, (*b*) 310 m, and (*c*) 610 m. The model uses a grid of 0.5° in the horizontal with 20 levels in the vertical. The same color bar is used for the three model levels. The regions of high variability will contribute directly to the variability of acoustic travel time in the simulations. The locations of these regions are in general agreement with those observed for sea surface height variability by Seasat altimetry [*Cheney et al.*, 1983].

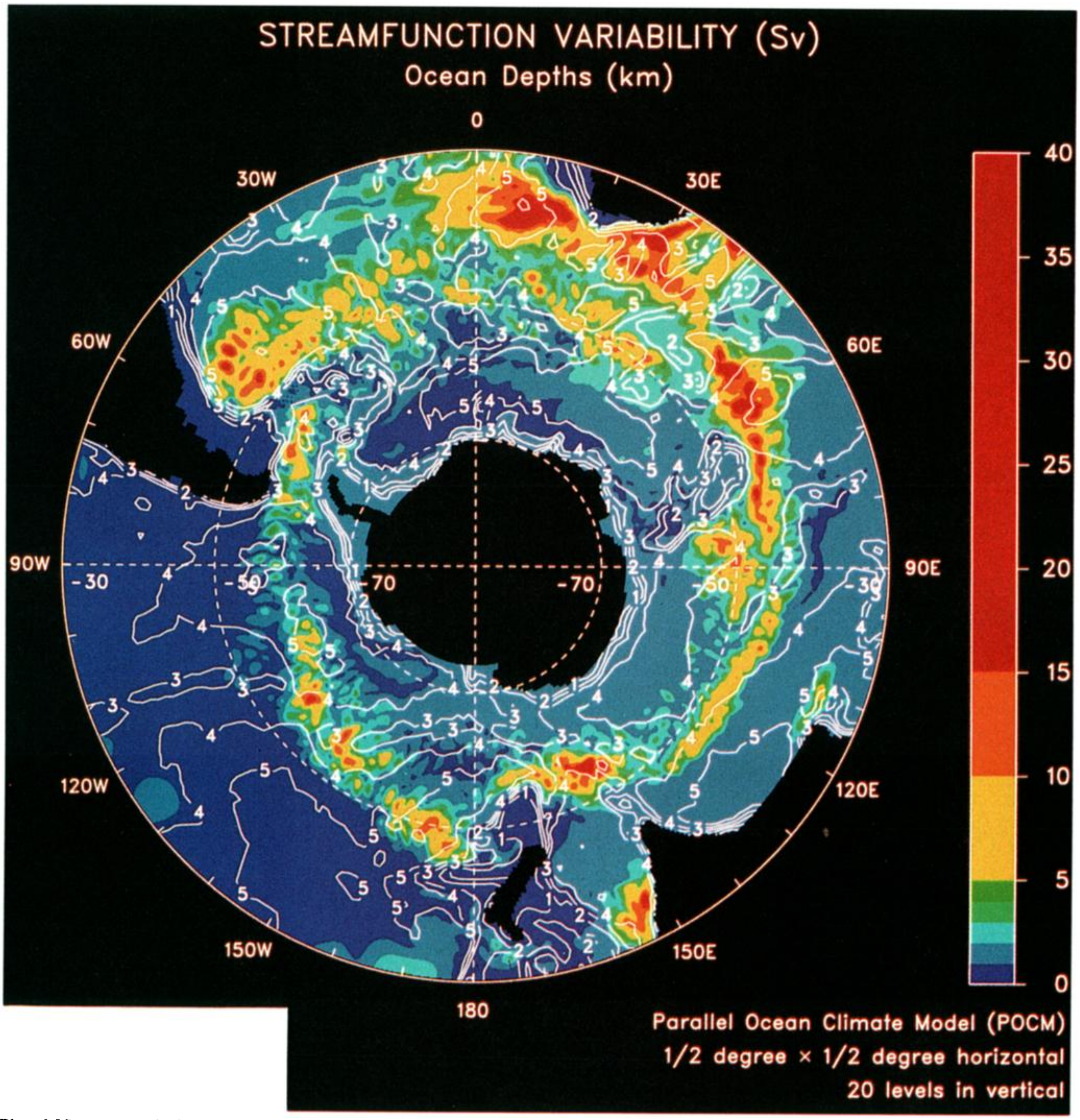

Plate 2 [*Semtner and Chervin*]. Standard deviation of modeled transport stream function for the same 2.5-year period as in Plate 1. Contour lines of model depth are added to show the dominant influence of topography on variability.